

Structure-function mimicry of oxidized purple acid phosphatase-PAP_{ox} – A new functional model

Shobha A Waghmode^{a,*}, Sadgopal K Date^b, Vidya S Gupta^c & Sandhya Y Rane^{d,*}

^aDepartment of Chemistry, Abasaheb Garware College, Pune 411 004, India

^bDepartment of Physics, University of Pune, Pune 411 007, India

^cPlant Molecular Biology, National Chemical Laboratory, Pune 411 008, India

^dDepartment of Chemistry, University of Pune, Pune 411 007, India

Email: syrane@chem.unipune.ernet.in

Received 27 October 2009; re-revised and accepted 21st July 2010

Electronic structure and spectroscopic properties of the novel diiron active site of oxidized mammalian purple acid phosphatase analogues, Fe-6: [Fe₂ (μ-O) (μ-OAc) (4HNSQ_{ox})²⁻ (ONSQ_{ox})²⁻ (H₂O)₄] and Fe-7: [Fe₂ (μ-O) (μ-OAc) (ONSQ_{ox})²⁻ (OAc) (H₂O)₄] are described. Magnetic susceptibility SQUID data of Fe-6 are best fitted to Heisenberg's isotropic spin pair ($S = 5/2, 3/2$) model using magnetic parameters $g = 2$ and $J = -36.8 \text{ cm}^{-1}$ with R factor = 6.4×10^{-4} . The antiferromagnetic exchange establishes Fe(III)-O-Fe(III) dimeric core with Fe(III) site having two radical ligations in the naphthoquinone oxime form of lawsone oxime. In the model compound Fe-7 of oxidized purple acid phosphatase, bridged and terminal acetate functions are identified according to their different energies of activations, i.e., ~34 and 58 kJ mol⁻¹ respectively. Also, the reduced naphthoquinone oxime form of ligand is characterized by its energy of activation (~15 kJ mol⁻¹) from pyrolytic reaction. Mössbauer parameters, $\delta = 0.4 \text{ mm s}^{-1}$ and $\Delta E_Q = 0.8 \text{ mm s}^{-1}$, are characteristics of oxidized Fe(III) in high spin octahedral site. Only Fe-6 shows analogous physiological DNA cleavage activity on pUC19 plasmid and acts as a good model of oxidized purple acid phosphatase enzyme.

Keywords: Bioinorganic chemistry, Nuclease activity, PAP_{ox} analogues, Iron, DNA cleavage, Antiferromagnetic exchange

IPC Code: Int. Cl.⁹ C07F15/02

Purple acid phosphatase (PAP) is a non-heme redox enzyme^{1,2} that catalyses the hydrolysis of phosphomonoesters at an optimum $pH < 7.0$. The hydrolytic activity of PAP enzyme corresponds to its physiological function³⁻⁵ such as DNA cleavage. The X-ray crystal structure of PAP enzyme from rat bone of mammalian origin⁶ reveals the distinct octahedral coordinations at the dinuclear iron center in its active site with two accessible oxidation states in the catalytically inactive oxidized form Fe(III)-μ(O)-Fe(III), (PAP_{ox}) and the catalytically active reduced form Fe(III)-μ(OH)-Fe(II), (PAP_r). Recently the model of PAP having a central bridging phenolate moiety with terminal phenolate ligands with asymmetric dinuclear complexation has been reported⁷. Although the nuclease activity of PAP is of prime importance in cancer chemotherapy, regulating gene expression and design of synthetic restriction enzyme such as structure-activity correlation in redox active PAP is least attempted in model compounds⁸⁻¹⁰.

Due to tyrosine →Fe(III) charge transfer transition at λ_{max} 500 nm, PAP exhibits a characteristic purple colour in its inactive oxidized Fe(III)-μ(O)-Fe(III) form (PAP_{ox}) and a pink colour at 510 nm in its active reduced form Fe(III)-μ(OH)-Fe(II) (PAP_r) which classified the enzyme as EC 3.1.3.2¹¹. However, the importance of such charge transfer with tyrosine cofactor is not yet clear¹²⁻¹⁴. It may be due to valence tautomeric¹⁵ behavior of active site which has been recently established with functional modelling of 'PAP_r' form¹⁶ using redox isomeric phthiocol oxime ligand¹⁷. This valence tautomeric mixed-valent Fe(III)-μ(OH)-Fe(II) model compound exhibited ~75 % nuclease activity of RAPase (reconstituted acid phosphatase). However, this model is devoid of acetate bridges, wherein "redox functioning" moieties in former structural models¹⁸ mimic bridged and terminal aspartates in octahedrally coordinated homodimeric iron site⁶. At the same time, the earlier reported functional models were also devoid of

bridged and terminal carboxylate ligands^{19,20} except for the only functional model of plant origin, kbPAP, with the Fe(III) $\mu(\text{OH})\text{Zn}(\text{II})$ active site reported by Neves *et al.*^{21,22} which contains the Fe(III) $(\mu\text{OAc})_2\text{Zn}(\text{II})$ core.

Recently, it has been reported that organic compounds inhibit the osteoporosis controlling activity of the enzyme, PAP²³. We have earlier shown that organic compounds like the vitamin K₃ family members (substituted naphthoquinone derivatives) can act as inhibitors of PAP enzyme with potential antioncogenic activity¹⁷. Some researchers²⁴⁻²⁶ have compared the bioinorganic approach in copper and iron metalloenzymes which deals with modelling of dinuclear metallosite of PAP^{27,28}. Bidentate ligands were thought to be capable of stabilizing the Fe₂ III,II and Fe₂ III,III forms and serve as an active site model of the PAP²⁹. Recently we have established the significance of metal cofactors in native APase of *Solanum tuberosum* (potato) in their bio-physiological functions⁵. At the same time the importance of organic cofactor as tyrosine radical at active dinuclear mixed valent iron site in APase of *Ipomoea batatas* (sweet potatoes) has been reported^{4a}. Inspired by such valence tautomeric non-innocent coordinations^{30,15} at active site of native PAP, we have used radical ligand of N^oO donor site, viz., lawsone oxime to study model compounds of PAP_{ox}. LwOx exhibits two coordinating valence tautomers, i.e., 2-oxido-1, 4- iminosemiquinone oxime (ONSQ_{ox})²⁻ and 4-hydroxy-1,2-iminosemiquinone oxime (4HNSQ_{ox})⁻. Due to intra- and intermolecular H-bondings, hydroxyl naphthoquinones and their oximes exhibit an intrinsic radical nature which has been established experimentally^{17,31} as well as theoretically^{32,33}. In continuation of such studies and to throw light on PAP metallo site in the present report, we have tested the PAP_{ox} site with model compounds, Fe-6 and Fe-7.

In the present work, we have studied the role of organic redox cofactors, particularly acetates and tyrosine, in the model compounds of PAP_{ox} with dinuclear iron site of mammalian origin. The valence tautomeric ligation generating phenoxyl radical as characteristic feature relevant to tyrosine function and μ -acetato diiron III,III core is mimicked in model compounds using redox susceptible ligand, viz., 2-OH 1,4-naphthoquinone oxime or lawsone oxime (LwOx)³¹. TG, VTMS, Mössbauer and EPR spectroscopic techniques have been used to study the iron core in non-innocent coordination. The study

reveals new physiological functional mimickry of PAP_{ox} form of active site which is rarely modelled in structural mimics²⁴ and thought to be inactive in native enzyme^{6,12} and also role of redox cofactors.

Materials and Methods

All the chemicals used in the preparation of metal complexes were of analytical grade. Lawsone (2-hydroxy-1,4-naphthoquinone) was obtained commercially from Sigma and used without purification. Solvents were distilled and dried according to the literature³⁴. Lawsone oxime (LwOx) was prepared according to procedure reported earlier³⁵.

Synthesis of Fe-6 and Fe-7

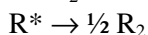
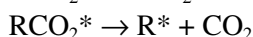
Iron powder (0.1 g) was mixed with 10 ml glacial acetic acid³⁶ and heated for 6 h at 80 °C. The precipitate of ferric acetate was filtered and washed with ether and dried in vacuum. Anal.: Calc. C, 30.93; H, 3.89; Fe, 34.27. Found: C, 30.18; H, 4.01; Fe, 34.43. Fe(OAc)₃ (1 mmol) was added to warm methanolic solution of lawsone oxime (LwOx, 1 mmol) with constant stirring for 1 h. The precipitated brown coloured chelate (Fe-6) was separated and washed successively with cold water and then with ether. The chelate was dried under vacuum at room temperature. [Anal.: Calc. Fe-6: C, 41.47; H, 3.95; N, 4.39; Fe, 25.10. Found: C, 39.84; H, 3.70; N, 3.87; Fe, 25.19]. For Fe-7, a similar procedure was followed with 1 mmol lawsone oxime and 2 mmol. Fe(OAc)₃. [Anal.: Calc. Fe-7: C, 33.16; H, 4.17; N, 2.76; Fe, 31.49. Found: C, 30.18; H, 3.97; N, 2.97; Fe, 33.91].

The chemical compositions of Fe-6 and Fe-7 were established from elemental analysis. C, H and N were determined using Elementar Vario EL analyzer. The compositions of the complexes were confirmed from TG studies of Fe-6 and Fe-7 on a laboratory constructed thermobalance, details of which were reported elsewhere³⁷. IR spectra of ligand and the iron complexes were recorded as Nujol mull on Perkin-Elmer FTIR (model 1600) infrared spectrometer at the Department of Chemistry, University of Pune. X-band EPR spectra of Fe-6 and Fe-7 were recorded on a Bruker EMX spectrometer at National Chemical Laboratory, Pune. Temperature dependant magnetic susceptibility of powdered sample Fe-6 was measured by using SQUID susceptometer (Quantum design) at 1.0 T in the range 2-300 K at Max-Planck Institute, Mülheim, Germany. The magnetic susceptibility was corrected for underlying diamagnetism using Pascal's constants.

⁵⁵Fe Mössbauer spectra of Fe-6 and Fe-7 were obtained on a Mössbauer spectrometer (5600, Austin, USA) at National Chemical Laboratory, Pune. Isomer shifts were referenced with respect to the metallic iron at 300 K. DNA cleavage reaction using pUC19 plasmid (300 ng) in tris buffer (pH = 8.0) was treated with Fe-6 and Fe-7 at 37 °C for 30 min. in the presence of H₂O₂ on 1 % agarose gel electrophoresis and tris acetate – EDTA buffer containing 0.5 µg ml⁻¹ ethidium bromide at 40 V for 2 h.

Results and Discussion

In compositional studies of Fe-6 and Fe-7, Fe(OAc)₃ provides CH₃COO⁻ by controlling the M:L ratio. Excess acetate ions in solution may act as reducing agent and may raise spin concentration on LwOx in its one-electron reduced NSQ_{ox} form during coordination¹⁷. From earlier reports¹⁸ such redox processes in modelling of PAP show involvement of dicarboxylate as reducing agent in complex, as follows:



Hence, instead of metal ion reduction, redox susceptible LwOx and dissolved oxygen may undergo reduction due to acetate function in Fe-6 and Fe-7 to yield complexes with following probable electronic structures: Fe-6: Fe₂(III, III)-(µ-O)(µ-OAc)(ONSQ_{ox})²⁺ (4HNSQ_{ox})⁺ (H₂O)₄, and Fe-7: Fe₂(III, III)(µ-O)(µ-OAc)(ONSQ_{ox})²⁺ (OAc) (H₂O)₄.

The stoichiometries of pyrolytic reactions of both complexes at different steps are ascertained in Table 1. Kinetic parameters are calculated from the dynamic TG curves (Fig. 1) using various expressions with the help of computer program developed in our

laboratory based on the rising temperature expression of Coats and Redfern. The energy of activation data for different functional groups shows three steps of decomposition for Fe-6 and two steps for Fe-7.

Fe-6 and Fe-7 complexes have the acetate groups in their coordination sphere. In the model compound Fe-7, bridged and terminal acetate functions are identified according to their different energies of activations, i. e., ~34 and 58 kJ mol⁻¹ respectively. Using *E*_a for non-interacting water molecule³⁸ (i.e. 2.8 kJ × 4 = 11.2 kJ for four H₂O) necessary for expulsion in first step of Fe-7, the energy required for loss of one OAc ligand is quantitized as 34.03 kJ mol⁻¹ OAc (45.23-11.20 = 34.03 kJ mol⁻¹).

We have reported earlier the reactivity of acyl and aquo groups in metal-quinone aggregates of photosystem II containing LwOx functional moieties; the acyl group in terminal ligation possesses an energy of 58 kJ mol⁻¹ in pyrolytic reaction³⁸. If the

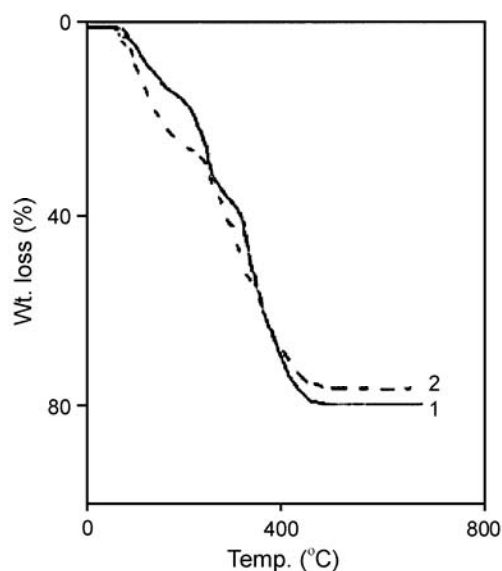


Fig. 1 — Thermograms of Fe-6 and Fe-7. [1, Fe-6 ; 2, Fe-7].

Table 1 — Activation energies of the complexes, Fe-6 and Fe-7 from dynamic TG

| Comp. | Step | Temp. (°C) | Mass losses (%) | Probable group lost | Residue | Order | <i>E</i> _a (kJ) | <i>E</i> _a (kJ mol ⁻¹) |
|-------|------|------------|----------------------------|------------------------------|---|-------|----------------------------|---|
| Fe-6 | I | 85-190 | 15.00 (15.93) ^a | 4H ₂ O + 0.5(OAc) | Fe ₂ (O)0.5 (OAc) ^b (LwOx) ₂ | 1.25 | 28.12 | 2.8/H ₂ O 33.84/OAc |
| | II | 200-310 | 20.50 (19.44) | 0.5(LwOx) + 0.5(OAc) | Fe ₂ (O) + 1.5 (LwOx) | - | - | - |
| | III | 310-500 | 44.20 (44.53) | 1.5(LwOx) | 2FeO | - | - | - |
| Fe-7 | I | 85-210 | 25.05 (25.84) | 4H ₂ O + (OAc) | Fe ₂ (O) (OAc) (LwOx) | 1.9 | 45.23 | 34.03/(OAc) |
| | II | 210-450 | 49.05 (48.95) | 1LwOx + (OAc) | 2FeO | 1.3 | 73.27 | 58/(OAc) 15.27/LwOx |

^aFigures in parenthesis indicate calculated values. ^bOAc = CH₃COO⁻.

second acetate ligand is considered in the terminal coordination in Fe-7 with 58 kJ mol^{-1} energy of activation, we can estimate the E_a value of the eliminated LwOx in the second step as $15.27 \text{ kJ mol}^{-1}$. This indicates that the acetate ligands in Fe-7 are of two types, viz., bridged (with $E_a \sim 34 \text{ kJ mol}^{-1}$) and terminal (with $E_a \sim 58 \text{ kJ mol}^{-1}$) with terminal LwOx in reduced NSQ_{ox} form³⁹. The E_a required for H₂O loss and OAc loss in first step of pyrolysis of Fe-6 are thus estimated as 2.8 kJ mol^{-1} H₂O and $33.84 \text{ kJ mol}^{-1}$ OAc, ($2.8 \times 4 + 33.84 \times 0.5 = 28.12 \text{ kJ}$ total E_a) indicating that the acetate ligand in Fe-6 may be in the bridged form.

The IR spectra of the NSQ_{ox} form shows the $\nu\text{C=O}$ frequencies below 1600 cm^{-1} as symmetric stretch absorptions³⁵ in Fe-6 and Fe-7 (Fig. 2). Such frequencies are seen in Fe-6 at 1584 cm^{-1} and in Fe-7 at 1586 cm^{-1} .

In LwOx, the IR band at 3500 cm^{-1} is assigned to intermolecular H-bonding in *syn*-form while medium band at 3189 cm^{-1} can support the weak intramolecular H-bonding in *amphi*-form⁴⁰. A weak but sharp absorption band at 3700 cm^{-1} in Fe-6 may be assigned to νOH of 4-OH- NSQ_{ox} form of LwOx which is absent in Fe-7. A broad band at $3370\text{--}3400 \text{ cm}^{-1}$ may be assigned to νOH stretching frequency of water molecules coupled with oximino hydroxyl groups. Antisymmetric stretch doublet at $\sim 830 \text{ cm}^{-1}$ and 849 cm^{-1} are seen in Fe-6 and Fe-7 suggesting Fe(III)–O–Fe(III) bridges in the respective complexes. Cannon⁴¹ and Que & True¹ have earlier

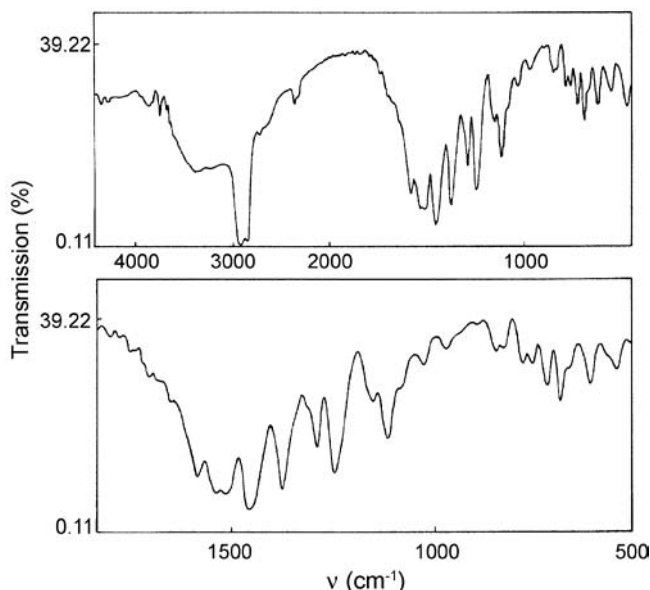
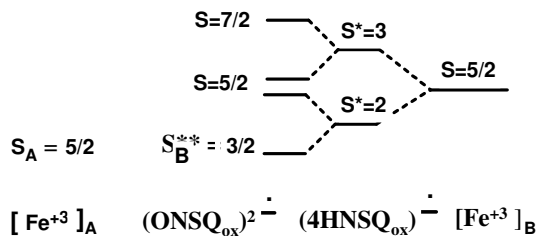


Fig. 2 — IR spectra of Fe-6.

reported a strong band at 604 cm^{-1} for $\pi(\text{COO})$ in the acetate bridged iron complex, which is shifted to 620 cm^{-1} in oxo and acetate complexes of iron. In both Fe-6 and Fe-7, such strong deformation modes are seen at 617 and 615 cm^{-1} .

TG and IR studies show that both Fe-6 and Fe-7 are dimers with μ -oxo and μ -acetato bridges. Magnetization studies of Fe-6 have been performed over the temperature range 2–290 K (Fig. 3). The magnetic moment observed at 290 K is 4.68 BM and decreases slowly to 3.03 BM at 80 K. It then decreases more rapidly to reach roughly 1.4 BM at 2 K. The $\chi_m^{\text{corr}}T$ also decreases with temperature indicating antiferromagnetically coupled $[\text{Fe}^{+3}]_A$ and $[\text{Fe}^{+3}]_B$ sites as shown in Scheme 1, generating resultant $S = 5/2, 3/2$ spin pair model at the active site of Fe-6.



S^* and S^{**} ground states generated after spin-spin coupling interactions

Scheme 1

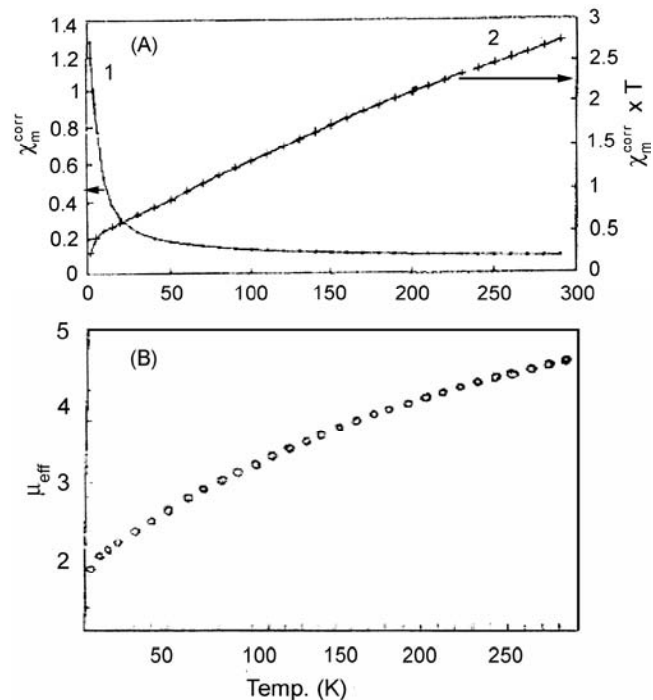


Fig. 3 — (A) VTMS plots of Fe-6. [Variation of (1) χ_m^{corr} with temperature; (2) $\chi_m^{\text{corr}} \times T$ with temperature. (B) Variation of magnetic moment (μ_{eff}) of Fe-6 with temperature.

Hence, $\chi_m^{\text{corr}} \times T$ data were best fitted by using HDVV spin pair $S = 5/2, 3/2$ model. The best fit parameters $J = -36.79 \text{ cm}^{-1}$, $g = 2.0$ were used (Fig. 3) with an agreement factor $R = 6.41 \times 10^{-4}$. Compared to our earlier reported model¹⁶ of PAP_r enzyme in reduced form where $J = -13.5 \text{ cm}^{-1}$, in the present study, the large exchange coupled constant for Fe-6 indicates Fe³⁺- $\mu(\text{O})$ -Fe³⁺ bridge instead of μOH bridge between [Fe³⁺]_A and [Fe³⁺]_B metallosites. In native oxidized enzyme PAP_{ox}, the Fe(III)- $\mu(\text{O})$ -Fe(III) core is reported to have J value^{42,43} ranging from ~ -40 to -150 cm^{-1} . Such high coupling constant in model compounds of non-heme active site have been reported by Weighardt and coworkers⁴⁴. Room temperature EPR of Fe-6 (not shown) shows very broad exchange coupled signal at $g = 2.16$. Mössbauer spectra with single quadrupole split signal at $\delta = 0.4 \text{ mm s}^{-1}$ with $\Delta E_Q = 0.8 \text{ mm s}^{-1}$ parameters support Fe(III) high spin octahedral configuration around both Fe(III)- $\mu(\text{O})$ -Fe(III) sites (Fig. 4). The above studies support an electronic structure of Fe-6 such as $[(\text{H}_2\text{O})_4\text{Fe(III)}(\mu\text{-O})(\mu\text{-OAc})\text{Fe(III)}(4\text{-OH-1,2-NSQ}_{\text{ox}})^-(2\text{-oxido-1,4-NSQ}_{\text{ox}})^{2-}]$.

The Fe-7 complex shows $5.45 \mu_{\text{eff}}$ per dimer or 3.85 BM/Fe^{3+} . TG and IR data indicate that one terminal ligand is coordinating in (2-oxido 1,4 NSQ_{ox})²⁻ form which generates $S^* = 5/2-1/2 = 2$ spin state at one Fe(III) high spin site similar to [Fe³⁺]_A site in PAP_r functional model¹⁶. Antiferromagnetic exchange via $\mu\text{-oxo}/\mu\text{-carboxylato}$ bridges may occur between $S = 5/2, 2$ spin pair resulting in lowering of magnetic moment as compared to spin only value of Fe(III) high spin complex⁴⁵. Since variable temperature

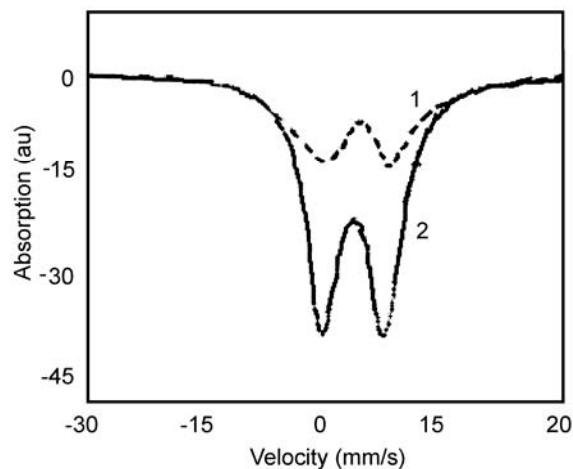


Fig. 4 — Mössbauer spectra of Fe-6 and Fe-7 at 300 K. [1, Fe-6; 2, Fe-7].

magnetic susceptibility data are not available for Fe-7 compound, we have compared the μ_{eff} of Fe-7, with that of Fe-6 at room temperature. The less reduction in μ_{eff} of Fe-7 compound as compared to that of Fe-6 is due to only one NSQ_{ox} ligation in Fe-7, while in Fe-6, two redox isomers in NSQ_{ox} forms are coordinating with [Fe³⁺]_B site (Fig. 5). Broad exchange coupled EPR signal at $g = 1.98$ is also characteristic of $S = 5/2, 2$ spin pair⁴⁶. A single doublet in Mössbauer spectrum of $\delta = 0.4 \text{ mm s}^{-1}$ with $\Delta E_Q = 0.78 \text{ mm s}^{-1}$ is characteristic of Fe(III) high spin configuration. From the above studies, we conclude that Fe-7 possesses the following electronic structure: $[(\text{H}_2\text{O})_4\text{Fe(III)}(\mu\text{-O})(\mu\text{-OAc})\text{Fe(III)}(\text{OAc})(2\text{-oxido-1,4-NSQ}_{\text{ox}})^{2-}]$. The probable electronic structures of Fe-6 and Fe-7 are shown in Fig. 5.

The mimicry of the hydrolytic cleavage functionality of native PAP^{4(b),5} was also studied by comparing DNA cleavage activity of radically coordinated $\mu\text{-oxo}/\mu\text{-acetate}$ iron dimers, viz., Fe-6 and Fe-7.

Fontecave *et al.*²⁵ have discussed the future investigations of hydrolytic cleavage of DNA by model compounds which suggest their biotechnological applicability in coming years. The physiological defense activity of native acid

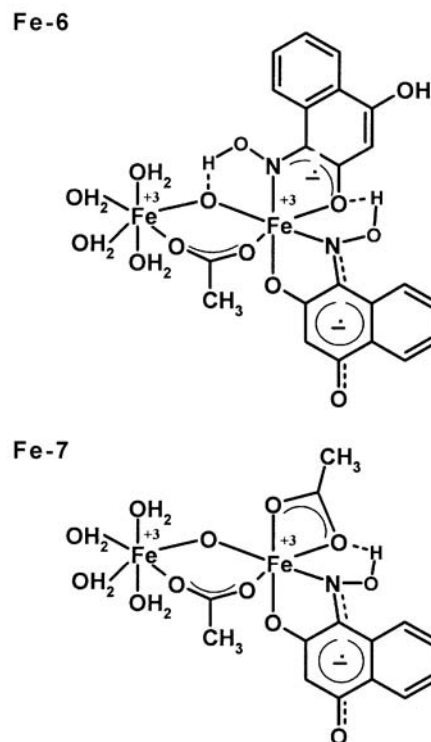


Fig. 5 — Electronic structures of Fe-6 and Fe-7.

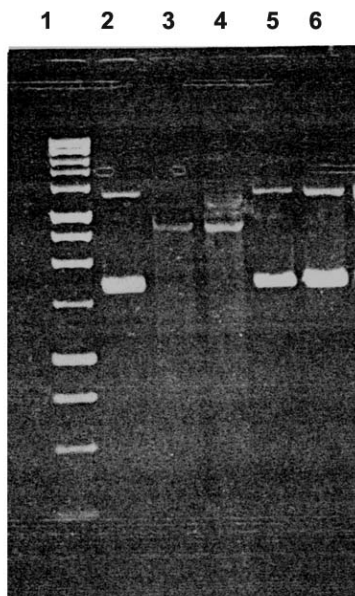


Fig. 6 — Nuclease activity of Fe-6 and Fe-7 on pUC 19 plasmid with H_2O_2 . [lane 1, marker; lane 2, pUC19 plasmid + H_2O_2 ; lane 3, Fe-6 (700 μM) + pUC19 plasmid + H_2O_2 ; lane 4, Fe-6 (500 μM) + pUC19 plasmid + H_2O_2 ; lane 5, Fe-7 (700 μM) + pUC19 plasmid + H_2O_2 ; lane 6, Fe-7 (500 μM) + pUC19 plasmid + H_2O_2].

phosphatase has been established in terms of its quantitative pUC-19 plasmid DNA cleavage activity⁵, together with reconstituted PAP_r model compounds¹⁶. Herein, the DNA cleavage activity of Fe-6 and Fe-7 complexes mimicking SOM assembly of PAP, have been studied using pUC19 plasmid DNA in presence of H_2O_2 (Fig. 6).

Fe-6 and Fe-7 are both homovalent having III, III oxidation states although only Fe-6 shows nuclease activity. We have reported earlier that oxo bridged diiron complexes, viz., $[Fe(Salen)]_2O$, cleave DNA more effectively compared to hydroxo-bridged $[Fe(Salox)_2OH]_2$ complex as the former is coordinatively unsaturated compared to latter⁴⁷. Also, compression of Fe(III)- $\mu(OH)$ -Fe(III) angle may prevent formation of HOO^- intermediate. Both Fe-6 and Fe-7 are μ -oxo/ μ -acetato bridged complexes but only Fe-6 cleaves DNA. Latour *et al.*¹⁸ have modelled associated redox processes in PAP. They have shown that carboxylate/di-phenyl phosphate exchange is strongly dependant on redox state of diiron centre and in the diferric complex, the reduction to mixed valent state occurs with ligand exchange. In the case of Fe-6, bridged acetate function may be replaced by 3'-5' phosphate function from DNA, while on removal of carboxylate, reduction of Fe(III) to Fe(II) may be taking place through an intermediate. Hydrophilicity of

NSQ_{ox} coordinated ligand may undergo PET (proton electron transfers) generating nucleophilic terminal OH ion on Fe(III) center. Oxidation potential may be decreasing at iron site due to replacement of terminal OH ligand in the form of H_2O by hydroperoxide ligand. Here, two electron transfers are associated with two redox active ligands in the first coordination sphere with evolution of two water molecules⁴⁸. Hence, the model Fe-6 complex mimics associated redox processes in PAP appropriately, while Fe-7 fails to cleave DNA plasmid because it has only one reduced NSQ_{ox} ligand in first coordination sphere.

Acknowledgement

SYR is grateful to the CSIR, New Delhi, India for financial support [No. 01(1686)/00/EMR-II]. The authors are also thankful to Dr Phalguni Chaudhari, Max-Plank-Institut fur Bioorganische Chemie, Mulheim, Germany, for providing facility of SQUID measurements.

References

- 1 Que L Jr & True A E, *Prog Inorg Chem*, 38 (1990) 97.
- 2 Yang Y S, McCormick J M & Soloman E I, *J Am Chem Soc*, 119 (1997) 11832.
- 3 Wilcox D E, *Chem Rev*, 96 (1996) 2435.
- 4 (a) Rane S Y, Shobha Dagade-Waghmode, Gupta V S, Khursheed Ah & Srinivas D, *Indian J Chem*, 41 (2000) 104; (b) Wang Z, Li-June Ming & L Que Jr, *Biochemistry*, 31 (1992) 5263.
- 5 Rane S Y, Badave K D & Khursheed Ahmed, *Indian J Chem*, 48A (2009) 15.
- 6 Lindquist Y, Johansson E, Kaija H, Vihko P & Schneider G, *J Mol Biol*, 291 (1999) 135.
- 7 Jarenmark M, Carlsson H & Nordlander E, *CR Chim*, 10 (2007) 433.
- 8 Francios V, Colette L, Marc F & Stephane M, *Inorg Chem*, 42(2) (2003) 499.
- 9 Than R, Feldmann A A & Krebs B, *Coord Chem Rev*, 182 (1999) 211.
- 10 Twitchett M B & Sykes A G, *Eur J Inorg Chem*, 2 (1999) 2105.
- 11 Wilcox M C, *Structure*, 4 (1996) 943.
- 12 Merks M & Averill B A, *Biochemistry*, 37 (1998) 11223.
- 13 Morokuwa K, Musaer D G, Vreven T, Basch H, Torrent M & Khoroshun D V, *IBM J Res Dev*, 45 (2002) 367.
- 14 Dietrich M, Munstermann D, Suerbaum H & Witzel H, *Eur J Biochem*, 199 (1991) 105.
- 15 Pierpont C G, *Coord Chem Rev*, 216 (2001) 99.
- 16 Salunke-Gawali S, Khursheed Ahmed, Varret F, Linares J, Zawre S, Date S & Rane S, *Hyperfine Interact*, 185 (2008) 47.
- 17 Rane S Y, Salunke-Gawali S, Khursheed Ahmed, Varret F, Linares J, Zawre S, Gonnade R, Srinivas D & Bhadbhade M, *J Mol Struct*, 892 (2008) 74.
- 18 Latour J M, Bernard E, Chardon Nobalt S & Deronzier A, *Inorg Chem*, 38 (1999) 190.

- 19 Albedyhl S, Averbuch-Pouchot M T, Belle C, Krebs B, Pierre J L, Saint-Aman E & Torelli S, *Eur J Inorg Chem*, 6 (2001) 1475.
- 20 Bois J D, Mizoguchi T J & Lippard S J, *Coord Chem Rev*, 200 (2000) 443.
- 21 Neves A, Lanznasster, Bortoluzzi A J, Peralta R A, Casellato A, Castellano E E, Herrald P, Riley M J & Schenk G, *J Am Chem Soc*, 129 (2007) 7486.
- 22 Lanznaster M, Neves A, Bortluzzi A J, Szpoganicz B & Schwingel E, *Inorg Chem*, 41 (2002) 5641.
- 23 McGeary R P, Vella P, Jeffrey Y W Mak, Guddat L W & Gerhard S, *Bioorg and Med Chem Lett*, 19 (2009) 163.
- 24 Nie H, Aubin S, Mashuta M S, Wu J, Richardson J F, Hendrickson D N & Buchanan R M, *Inorg Chem*, 34 (1995) 2382.
- 25 Fontecave M, Menage S & Toia C D, *Coord Chem Rev*, 178-180 (1998) 1555.
- 26 Bernard E, Moneta W, Laugier J, Tuchagues J P & Latour J M, *Angew Chem Int Ed Engl*, 33 (1994) 887.
- 27 Adolfo Horn Jr, Ivo Vencato, Adailton J, Bortoluzzi, Rosmari Horner, Rene N Nome Silva, Bruno Spoganicz, Valderes Drago, Terenzi H & Oliveira M, *Inorg Chim Acta*, 358 (2005) 339.
- 28 Adolfo Horn Jr, Ivo Vencato, Adailton J, Bortoluzzi, Rosmari Horner, Rene N Nome Silva, Bruno Spoganicz, Valderes Drago, Terenzi H & Oliveira M, *Inorg Chem Comm*, 4 (2001) 388.
- 29 Paredes-Garcia, Venegas-Yazigi D & Latorre R O, *Polyhedron*, 25 (2006) 2026.
- 30 Pierpont C G, *Coord Chem Rev*, 219 (2001) 451.
- 31 Todkary A V, Dalvi R, Salunke-Gawali S, Khursheed Ahmed, Varret F, Linares J, Rane S, Yakhmi J V, Bhadbhade M, Srinivas D & Gejji S P, *Spectrochim Acta Part A*, 63 (2006) 130.
- 32 Dhumal N R, Todkary A V, Gejji S P & Rane S Y, *Theo Chem Acc*, 113 (2005) 167.
- 33 Joshi K A, Thube D R, Rane S Y & Gejji S P, *Theo Chem Acc*, 110 (2003) 322.
- 34 Perrin D D, Armargo W L F & Perrin D R, *Purification of Laboratory Chemicals*, (Pergamon, London) 1966; Pierpont C G, *Coord Chem Rev*, 219 (2001) 451.
- 35 Rane S Y, Padhye S B, Khan E M & Garge P L, *Synth React Inorg Met Org Chem*, 18 (1988) 609.
- 36 Jolly W L, *Synthetic Inorganic Chemistry*, Vol. 4, (Prentice-Hall, Inc, Englewood Cliffs NJ) 1960.
- 37 Salunke-Gawali S, Khursheed Ahmed & Rane S Y, *J Therm Anal Cal*, 76 (2004) 801.
- 38 Rane S Y, Salvekar J P, Dass N V R, Kaduskar P S & Bakare P P, *Thermochim Acta*, 191 (1991) 255.
- 39 Rane S Y, Padhye S B, Natu G N, Kumar A H & Khan E M, *J Therm Anal*, 35 (1989) 2331.
- 40 Rane S Y, Davale D D, Mulay M P & Khan E M, *Spectrochim Acta*, 46 A (1990) 113.
- 41 Cannon R D, *Inorg Chem*, 37 (1998) 1913.
- 42 Que L Jr, *ACS Symp Ser*, 372 (1998) 152.
- 43 Vincent J B, Olivier-Lilley Q L & Averill B A, *Chem Rev*, 90 (1990) 1447.
- 44 Wiegardt K & Weyhermuller C, *J Biol Inorg Chem*, 3 (1998) 96.
- 45 Tuchagues J P & Henrickson D N, *J Am Chem Soc*, 22 (1983) 2545.
- 46 Kurtz D M Jr, *Chem Rev*, 90 (1990) 585.
- 47 Rane S Y, Khumbhar A S, Damle S G & Dasgupta S T, *J Chem Res*, 51 (1999) 98.
- 48 Krebs B & Klabunde T, *Struct Bond*, 89 (1997) 178.